



# Experimental and numerical investigation on SiC coating delamination from C/SiC composites



Jingmin Jia <sup>a,b</sup>, Xufei Fang <sup>a,b</sup>, Weixu Zhang <sup>c,\*</sup>, Xue Feng <sup>a,b,\*</sup>

<sup>a</sup> AML, Department of Engineering Mechanics, Tsinghua University, Beijing 100084, China

<sup>b</sup> Center for Mechanics and Materials, Tsinghua University, Beijing 100084, China

<sup>c</sup> State Key Laboratory for Strength and Vibration of Mechanical Structures, Department of Engineering Mechanics, Xi'an Jiaotong University, Xi'an 710049, China

## ARTICLE INFO

### Article history:

Received 16 September 2013

Received in revised form 19 January 2015

Accepted 16 February 2015

Available online 21 February 2015

### Keywords:

A. Coating

B. Delamination

B. Fracture

Flexural test

C. Finite element analysis

## ABSTRACT

The delamination of SiC coating on C/SiC composites leads to severe oxidation of the carbon fibers and causes reliability problems of these composites during service. In this study, flexural test was conducted at room temperature to analyze the delamination behavior of SiC coating deposited on C/SiC substrate and finite element method (FEM) was adopted to simulate the interfacial crack between the SiC coating and the C/SiC substrate based on the experimental results. Results show that the fiber orientation has significant influence on the delamination of surface SiC coating. When the SiC coating is deposited parallel to the fiber orientation and interfacial delamination direction is along fiber direction, once delamination occurs, it inclines to propagate. However, when coating is prepared in other directions, the delamination inclines to be creased. The present analyses show that a proper combination of different fiber orientations can decrease the delamination of coating for better service of the materials in applications.

© 2015 Elsevier Ltd. All rights reserved.

## 1. Introduction

Carbon fiber reinforced silicon carbide (C/SiC) composites are important materials in aerospace and automobile industry, due to their high strength and superior fracture toughness in high temperature [1,2]. However, oxidation of C/SiC composites in high-temperature environment is still a key problem because the non-negligible porosity, internal and external multi-cracks exist in C/SiC substrate. To further enhance the anti-oxidation and the high temperature limit of C/SiC composites, a silicon carbide (SiC) coating is fabricated by chemically-vapor-deposition (CVD) on the surface of C/SiC composites. The SiC is an ideally promising coating for the C/SiC composites. During service, the silica formed at high temperature has a small diffusivity of oxygen and it can also seal the microcracks in coating and thus retard the further oxidation process of composites [2–5].

However, during service, especially in a sudden cooling process, the SiC coating may delaminate because of residual stress induced by the mechanical property difference and mismatch of thermal expansion coefficients between the coating and substrate. The delamination of SiC coating leads to the oxidation of the carbon

fiber and even the catastrophic damage of composites finally. It is one dominant factor causing reliability problems of C/SiC composites [6].

Therefore, the degradation of the coating that results from tensile or compressive stress generated in practical applications including thermal cycling process is of major concern and the mechanisms of coating delamination and failure are worth studying under controlled experimental conditions. Fang et al. developed three point bending test stage integrated with high speed camera for high temperature environment and realized real time observation of the surface coating spalling from substrate of C/SiC composites at 1400 °C [7]. However, the mechanism based on fracture mechanics for the delamination is not yet revealed. Particularly, C/SiC composites are prepared by chemical vapor infiltration (CVI) in which the preforms are fabricated to the 3-dimensional braid procedure and the composites are anisotropic materials. The orientation of fibers dominates the elastic property of composites and has a significant effect on the delamination of SiC coating. The effect of anisotropy of properties of C/SiC composites on the delamination of SiC coating is of great value for optimizing the application of C/SiC composites, which however, is still unclear.

In this paper, flexural test at room temperature is used to analyze the delamination behavior of SiC coating deposited on C/SiC substrate. Based on the experimental results, a computational

\* Corresponding authors at: AML, Department of Engineering Mechanics, Tsinghua University, Beijing 100084, China.

E-mail addresses: [zhangwx@xjtu.edu.cn](mailto:zhangwx@xjtu.edu.cn) (W. Zhang), [fengxue@tsinghua.edu.cn](mailto:fengxue@tsinghua.edu.cn) (X. Feng).

analysis of a coated composite material under loading is conducted, in which material failure at the interface between the substrate and coating under loading is analyzed. The coating/substrate system which is taken into consideration consists of a C/SiC composite with varied fiber arrangements (orientations) and a SiC coating on it. In addition, the interfacial crack between the C/SiC substrate and the SiC coating is modeled. The purpose of the study is to determine the influence of the arrangement of carbon fiber as well as the coating thickness on the interfacial delamination and the driving force for the propagation of the interfacial crack.

## 2. Experiment

The present experiment focused on the delamination pattern of SiC coating on the C/SiC composite substrate with different fiber orientations. A bulk of 3D needled C/SiC composite was prepared by chemical vapor infiltration (CVI), then specimens with size of  $3\text{ mm} \times 4\text{ mm} \times 40\text{ mm}$  were cut from the fabricated composite and a monolayer SiC coating with a thickness of about  $10\text{ }\mu\text{m}$  was deposited on the composite surface by chemical vapor deposition (CVD). Three point bending tests were conducted by using an electronically controlled universal testing machine with a specimen span of 30 mm and a cross-head speed of 0.5 mm/min, as illustrated in Fig. 1(a). Surface morphology of the bottom surfaces of the specimens were characterized using field emission scanning electron microscope (SEM) after fracture failure.

Two typical curves of the load–deflection for SiC coated C/SiC composites are plotted in Fig. 1(b). The curves can be divided into two stages: the first stage ranges from the initial loading to the peak load and it shows in both curves that the composite has a linear elastic behavior. In the second stage after the peak load, apparent differences of the curves appear. The curve obtained from test 1 (black line) shows a rapid decrease of load after the peak load, which reflects a characteristic brittle fracture of the material. But in curve 2 a step-like behavior after the maximum flexural loading indicates crack deflection and fiber pulling out [8]. Experimental results also validate this analysis that the differences of these two flexural behaviors are due to the fiber orientations within the composite substrate, as directly illustrated by the SEM images in Fig. 2. In Fig. 2(a and b) there is no fiber pulling out since the fiber orientation is parallel to the cross section of the specimen, while in Fig. 2(c and d) clear fiber pulling out could be seen, and the fibers were arranged parallel to the longitudinal direction of the specimen. The layered fiber arrangement in Fig. 2(c and d) also corresponds to the step-like stages in the load–deflection curve.

Furthermore, Fig. 3 shows multiple cracks perpendicular to the C/SiC substrate and the spallation of coating; the cracks emerge in the SiC coating when the specimens are subjected to the bending force, and then the coating delaminated along the interface. From Fig. 3 one can see that when the coating deposited parallel to the fiber, a large amount of coatings spalled off the substrate under surface tension, i.e., under bending. In Fig. 4, the channel cracks observed on the surface do not penetrate the substrate, but turn to run parallel to the substrate, inducing the spallation of the coating. It can also be observed that the fiber arrangement in the substrate, i.e., the fiber orientation (as illustrated in Fig. 5), has strong effect on the delamination of coating. Most part of the coating delaminated when it is parallel to the fiber, however, comparable small amount of coating delaminated when it is perpendicular to the fiber, which indicates the mechanisms of interfacial fracture are different. During service, the stress generated due to the elastic mismatch between the coating and substrate with different fiber directions plays an important role in the degradation of the SiC coating. Theoretically, when the interfacial energy release rate is higher than the interface fracture toughness, the interfacial crack would grow, causing spallation of the coating from the substrate. In the present experiments, no plastic deformation was observed, and the fracture is brittle. In the following section, theoretical and numerical analysis on the coating spallation with respect to the fiber orientation is presented.

## 3. Theoretical and numerical analysis

### 3.1. 2D plane strain model for the coating/substrate system

In this section, we established a 2D plane strain model for interfacial crack of SiC coated C/SiC composites.

The models of fiber orientations are established in Fig. 5(b) based on microscopic observation results (see the morphologies at top in Fig. 5(a)). Material properties of carbon fiber and SiC from literatures [9,10] are adopted and a micromechanical model is used to calculate properties of C/SiC substrate, which is simplified into an unidirectional fiber-reinforced composite in this study. Micromechanics equations for the longitudinal and transverse mechanical properties of the unidirectional fiber-reinforced composite have been summarized by Chamis [11]. For a unidirectional C/SiC substrate, the modulus in the longitudinal direction is

$$E_1 = E_1^f V_f + E^m (1 - V_f) \quad (1)$$

and the transverse modulus is

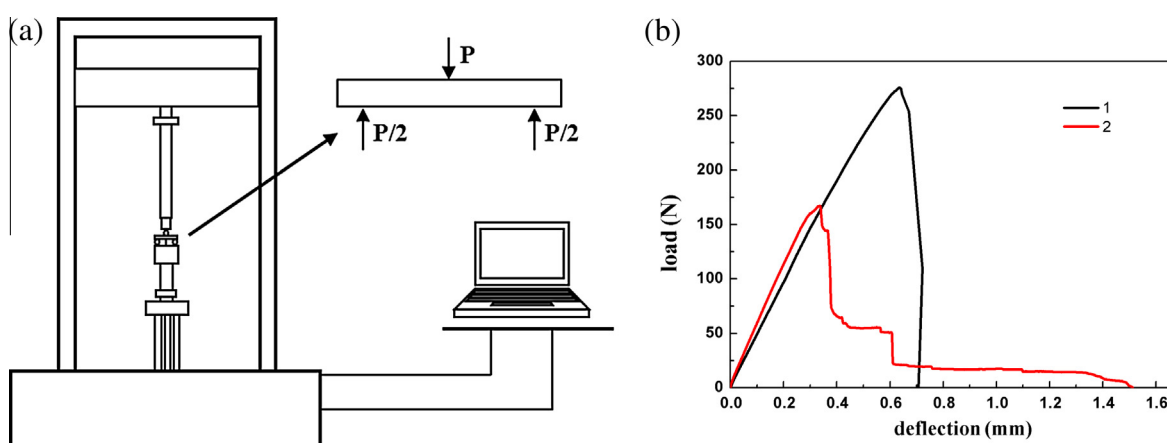


**Fig. 1.** (a) Schematic of three point bending test and (b) typical load vs. deflection curves.

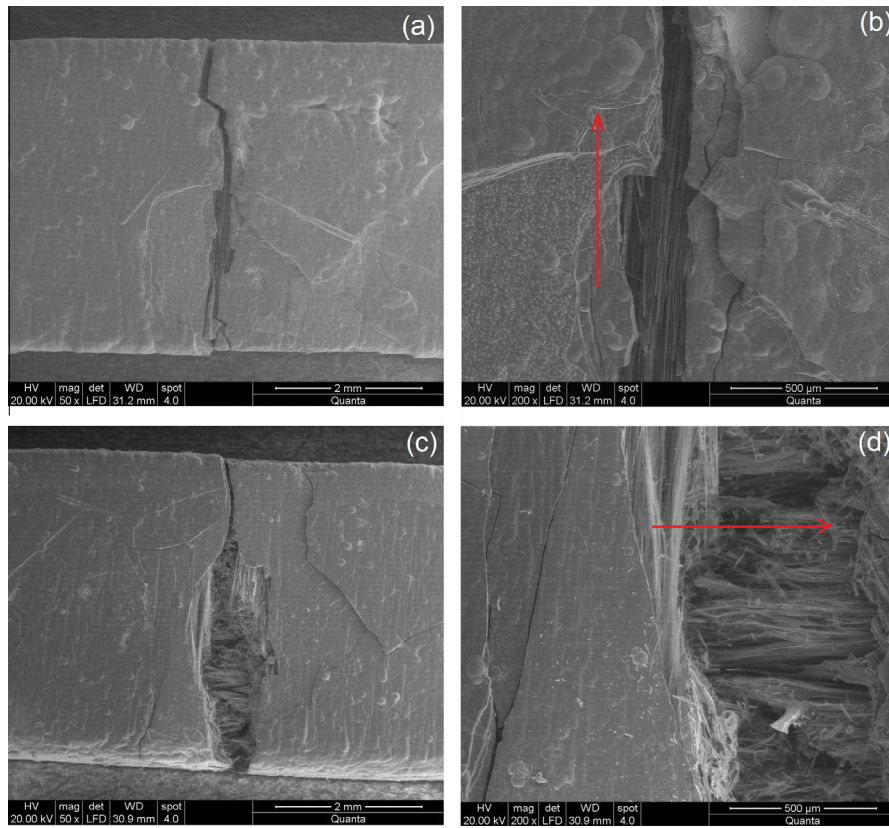


**Fig. 2.** Fiber orientation influences the load–deflection curves: (a and b) correspond to test 1 in Fig. 1; (c and d) correspond to test 2 in Fig. 1. Red arrows indicate the fiber orientations. (For interpretation of the references to colour in this figure legend, the reader is referred to the web version of this article.)

$$E_2 = \frac{E^m}{1 - \sqrt{V_f}(1 - E^m/E_2^f)} = E_3, \quad (2)$$

The expressions for shear modulus are

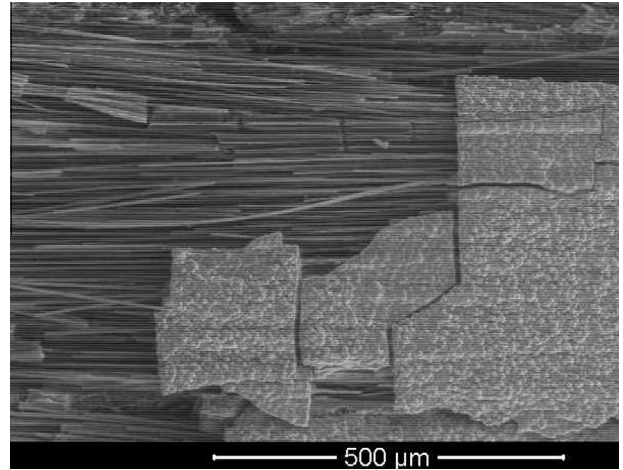
$$\begin{aligned} G_{12} = G_{13} &= \frac{G^m}{1 - \sqrt{V_f}(1 - G^m/G_{12}^f)}, \quad G_{23} \\ &= \frac{G^m}{1 - \sqrt{V_f}(1 - G^m/G_{23}^f)} \end{aligned} \quad (3)$$

and Poisson's ratios are

$$\begin{aligned} \nu_{12} = \nu_{13} &= \nu_{12}^f V_f + \nu^m V_m = \nu_{12}^f V_f + \nu^m (1 - V_f), \quad G_{23} \\ &= E_2 / (2 + 2\nu_{23}) \end{aligned} \quad (4)$$

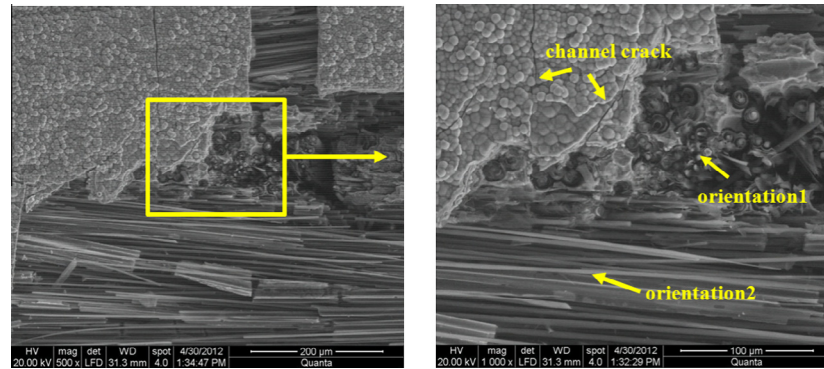
where  $E$  is elastic modulus;  $G$  shear modulus;  $V$  the fiber volume fraction, which is taken to be 45% in this study;  $\nu$  is Poisson's ratio and the subscripts  $f$  and  $m$  refer to properties of carbon fiber and SiC matrix, respectively. The subscripts 1, 2 and 3 are axes coordinates of representative volume element, as shown in Fig. 6. The material properties for transversely isotropic carbon fiber, isotropic SiC and transversely isotropic C/SiC are summarized in Table 1. The elastic moduli indicate that the brittle SiC coating is deposited on a relatively compliant substrate.

Fig. 7 shows the multiple channel cracks with symmetric interfacial crack, the simplified model is established to represent the bottom surface (which is subjected to tensile stress during flexural test) of the specimen based on the observation illustrated in Fig. 3. The rectangular area indicated by dotted line in Fig. 7 is extracted as a finite element method (FEM) model and is illustrated in Fig. 8 where the C/SiC substrate has a thickness of  $H$  with the SiC coating has a thickness of  $h$  on one side of the substrate. Due to symmetry,



**Fig. 3.** The multiple channel cracks of SiC coating.

only a representative unit part of the coating/substrate system is modeled along with proper boundary conditions. An edge-type crack with length  $a$  is assumed. In the calculation we set  $H = W = 2.4$  mm, while the coating thickness  $h$  and the crack length  $a$  are set as variables. A uniform normal displacement ( $u = 0.0006$  mm) is prescribed onto the right edge of the integrated structure based on the three-point bending test. Symmetry boundary conditions are imposed at the left edge of substrate and the bottom surface,  $u_x = 0$  at  $[x = 0, 0 \leq y \leq H]$  and  $u_y = 0$  at  $[y = 0, 0 \leq x \leq W]$ . The interface of interest is the one between the substrate and the coating. In general, the steady-state energy release



**Fig. 4.** SEM surface morphologies of the SiC coating after spallation failure subjected to three point bending test.

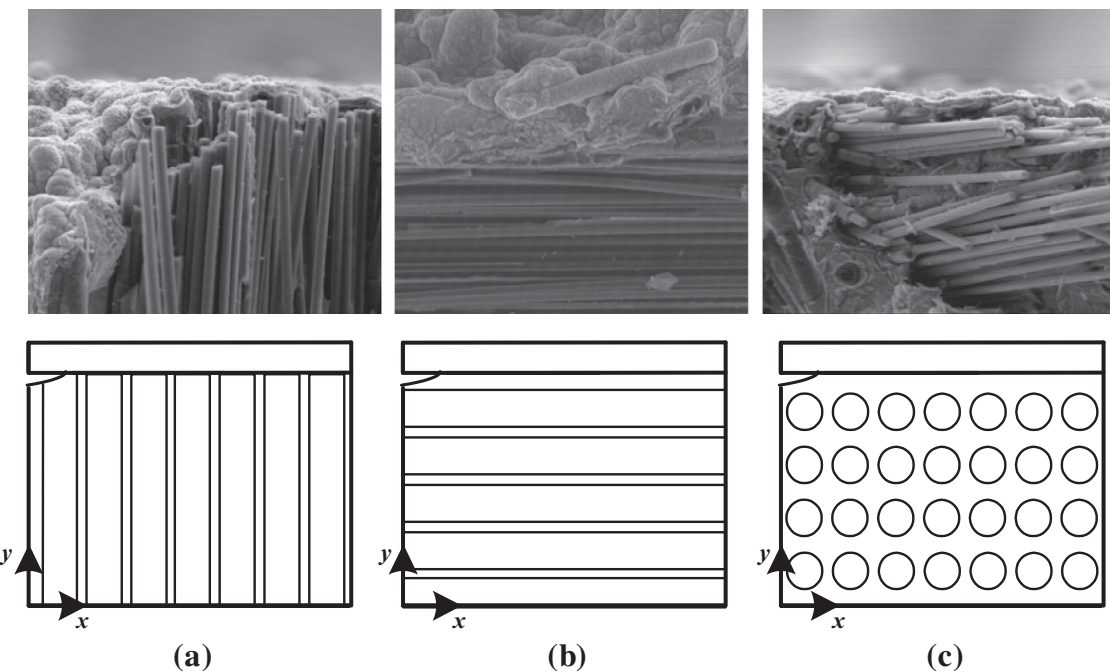


**Fig. 5.** Three types of carbon fiber orientations in the substrate with respect to the coating: (a) orientation-I, the longitudinal direction of the carbon fiber is perpendicular to the interface crack and along the y axis. (b) Orientation-II, the longitudinal direction is parallel to the interface and along the x axis. (c) Orientation-III, the longitudinal direction is perpendicular to the interface and along the z axis.

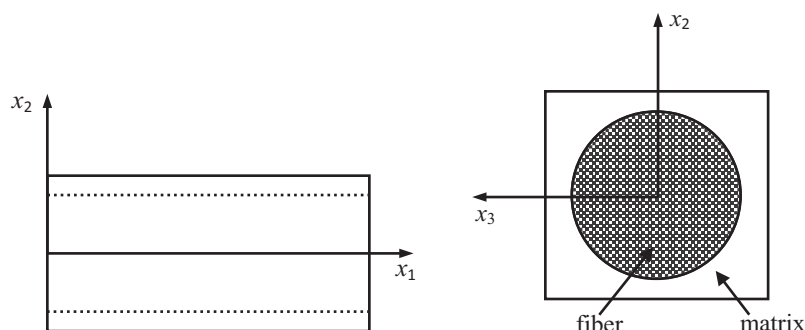


**Fig. 6.** Simplified representative volume element representing a fiber (*f*) and surrounding matrix (*m*) in a unidirectional fiber-reinforced composite.

rate of interfacial crack can be calculated from a 2D plane strain model. So we consider the steady-state propagation of the crack. The finite element software Abaqus is used in the present work

and the method of *J*-integral is adopted for the calculation of the interfacial energy release rate, since the fracture is brittle and linear elastic.

**Table 1**

Material properties at room temperature [9,10].

Materials	Young's modulus (GPa)		Shear modulus (GPa)		Poisson's ratio in plane axial	
	$E_1$	$E_2$	$G_{12}$	$G_{23}$	$\nu_{12}$	$\nu_{23}$
Carbon fiber (T300)	220	22	4.8	7.75	0.12	0.42
SiC matrix/coating	430	430	180	180	0.2	0.2
Substrate	335.5	32	7	11.32	0.164	0.42

### 3.2. Fracture parameters

Here we focus on the delamination of SiC coating on an anisotropic C/SiC composite material in this study. For interfacial crack problems with anisotropic materials, the widely used fracture criterion is the energy release rate criterion, which is based on energy analysis.

Suo [12] carried out a theoretical analysis for interface fracture problems for anisotropic materials, and related the energy release rate  $G$  and stress intensity factor  $K$  for semi-infinite crack. However, for anisotropic material, the stress intensity factor  $K$  and the energy release rate  $G$  depend not only on the material properties, but also on geometry and external loads. It is a complex process to derive  $K$  and  $G$  for an arbitrarily general case and only under some particularly simple conditions such as the interfacial cracks in semi-infinite media can we get the expressions about  $K$  and  $G$ . However, external loads and boundary conditions are usually simple in composite materials' working environment, as simplified and illustrated in Fig. 8. From an energy standpoint, when studying the interface failure problems of composites such as factors that influence interfacial crack growth, some complex anisotropic problems can be simplified by analyzing  $G$  and  $J$  integral and as a result, it is not necessary to find out the values of loading phases and the  $K$ . Since the  $J$  integral (i.e. the value of  $G$  for linear elastic fracture) for an interfacial crack can be easily obtained by employing finite element methods, problems about interfacial cracks can be analyzed by using fracture mechanics based on the energy criterion as mentioned above.

For two-dimensional problems,  $J$  is expressed as [13]

$$J = \int_{\Gamma} \left( w dx_2 - \mathbf{t} \cdot \frac{\partial \mathbf{u}}{\partial x_1} ds \right) \quad (5)$$

where  $w = w(x_1, x_2)$  is the strain energy density,  $x_1, x_2$  are the Cartesian coordinates shown in Fig. 9.  $\Gamma$  is a closed counter-clockwise contour surrounding the crack tip,  $\mathbf{t} = \mathbf{n} \cdot \boldsymbol{\sigma}$  is the traction vector,  $\mathbf{n}$  is the normal to the curve  $\Gamma$ ,  $\boldsymbol{\sigma}$  is the Cauchy stress tensor, and  $\mathbf{u}$  is the displacement vector.

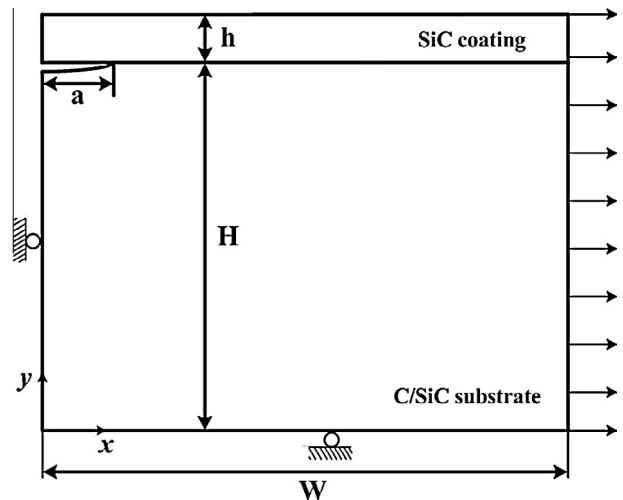


Fig. 8. Finite element model of the 2D steady-state interfacial crack.

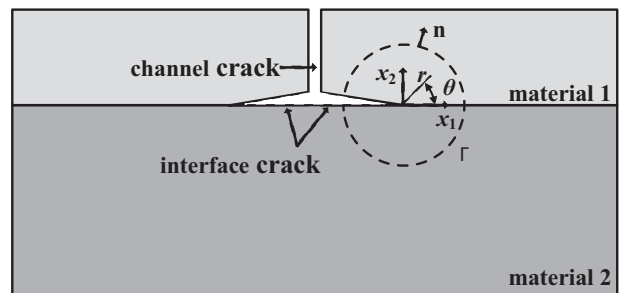


Fig. 9. Crack problem in bimaterial structure.

## 4. Results and discussion

When the tension applied to SiC coating is greater than its tensile strength, periodic surface crack forms (without delamination yet), which usually has little influence on coating functions since the molten silica can seal the cracks in high temperature. If the stress induces a continuous extension of interfacial delamination, the SiC coating will spall off the substrate, which has a significant influence on the composites due to the further serious oxidation of the substrate and fibers in the matrix [2]. From the viewpoint of fracture mechanics, the spallation of coating means the fracture driving force is continuously larger than interfacial toughness,

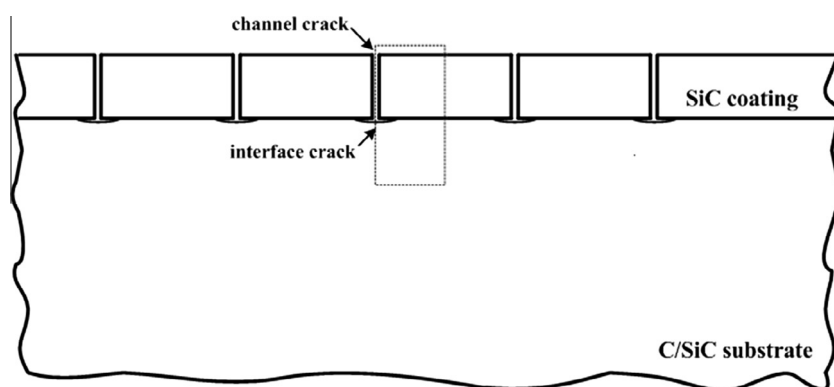
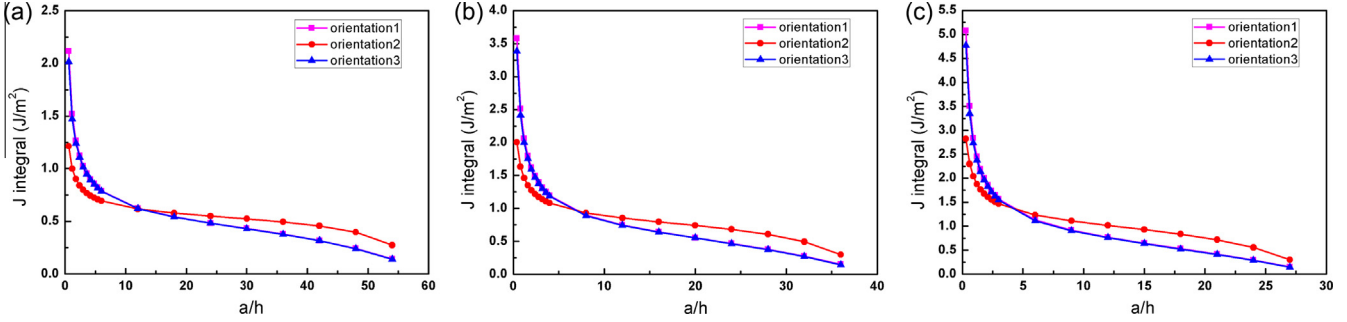
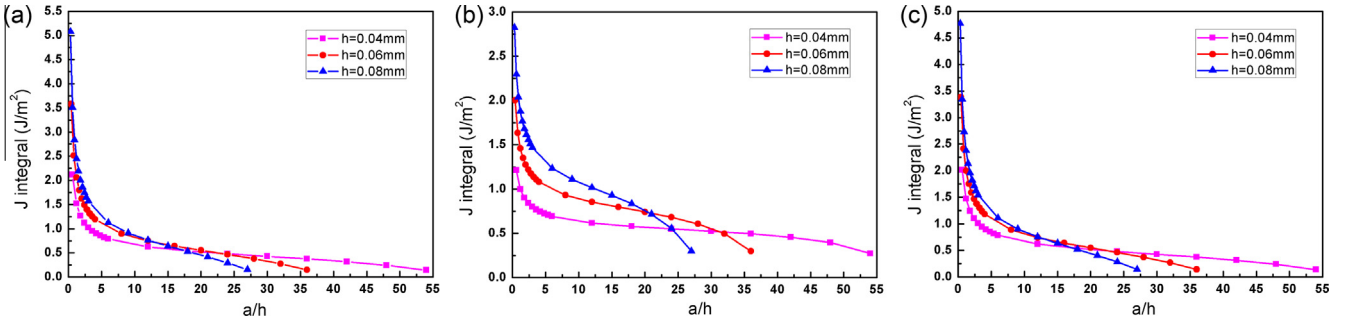


Fig. 7. Schematic of the coating/substrate system of multiple channel cracks with symmetric interfacial crack.



**Fig. 10.** The influences of fiber arrangements on the interfacial energy release rate, i.e., the  $J$  integral: (a)  $h = 0.04$  mm, (b)  $h = 0.06$  mm and (c)  $h = 0.08$  mm.



**Fig. 11.** The influences of the thickness of the SiC coating on the interfacial energy release rate, i.e., the  $J$  integral: (a) orientation-I, (b) orientation-II, and (c) orientation-III.

i.e.,  $G \geq G_c$ . The coating delamination will finally stop if the fracture driving force decreases rapidly and soon be smaller than the interfacial toughness with the propagation of delamination. Figs. 3 and 4 indicate that SiC coatings deposited on the surface of composite with different fiber orientations show different delamination behaviors. The coating deposited parallel to the fiber orientation is much easier to spall off the substrate than that perpendicular to the fiber orientation.

In Fig. 10, the energy release rate is plotted as a function of the normalized crack length  $a/h$  for various fiber geometric orientations. The numerical results show that the  $J$ -integral monotonically decreases as the crack length increases, the decrease of the  $J$ -integral is nonlinear and the decreasing rate becomes smaller as the crack length increases. The curve for orientation-I coincides with the one for orientation-III, indicating that the two kinds of fiber arrangements have identical influence on interfacial energy release rate. Elastic moduli along the loading direction for orientation-I and -III are equal because of the transverse isotropy of properties of C/SiC substrate. This resulted in identical energy release rate calculated. The descending trend of  $J$  integral for orientation-I and -III can be divided into two stages, the energy release rate for orientation-I is larger than that for orientation-II with the same crack length at the initial stage. However, at the second stage the energy release rate for orientation-I becomes smaller than that for orientation-II when the normalized crack length reaches a critical value, as the  $J$  integral for orientation-I decreases more rapidly with the increase of crack length. It can be observed that the existence of these two stages is independent on coating thickness, which explicitly illustrates that the interfacial crack for orientation-I is more prone to generate than that for orientation-II at the initial stage, but it may be arrested earlier than the crack for orientation-II at the second stage, which can be validated by the SEM observation in Fig. 3. The ratio of the coating elastic modulus to substrate modulus along the loading direction for orientation-I is greater than that for orientation-II, in other words, the coating is

relatively stiffer for orientation-I. It should be noticed that the multiple cracks illustrated in Fig. 7 would influence each other, the stiffer the coating is the stronger the influence of interaction between cracks on the energy release rate would become, leading to a more rapid decrease of the  $J$  integral.

In Fig. 11, the energy release rate is plotted as a function of the normalized crack length  $a/h$  for various coating thickness. For a given coating/substrate structure, the finite element calculations show that the  $J$  integral decreases monotonically and nonlinearly as the delamination width  $a$  increases. From Fig. 11, it can be seen that the interfacial energy release rate is larger for thicker coating at the initial stage of the crack propagation for all three orientations. However, the energy release rate becomes smaller for thicker coating when the normalized crack length exceeds a threshold value. The reason for this phenomenon is that the thicker the coating is, the faster the interfacial energy release rate decreases. Considering the fact that the multiple cracks in a stiff coating on a relatively compliant substrate, the interference between the multiple cracks affects the energy release rate directly, and the interaction becomes more and more prominent with the increasing of coating thickness, which leads to the rapid decreasing of the interfacial energy release rate.

Coating completely spalls off the substrate means  $G \geq G_c$  in the whole process. From experimental results shown in Figs. 2 and 3, one can see coating with respect to fiber orientation-II is easier to completely spall. Meanwhile, from Figs. 10 and 11, there is a slow downward stage in the curve of energy release rate in orientation-II. Combining the experimental and numerical results, once the interfacial delamination begins to propagate, it is difficult to stop for the coating with respect to orientation-II. However, the curve corresponding to orientation-I is more rapidly downward (i.e. with a steeper slope), and even the interfacial delamination begins to propagate, it will soon stop. The present analyses show that, in application, a suitable combination of different fiber orientations can decrease the delamination of coating for better service.

## 5. Summary and conclusions

The delamination of SiC coating on C/SiC composites is analyzed by experimental observation and numerical simulation. Results show that no plastic deformation occurred in the composite fracture and the linear elastic fracture mechanics can be used to analyze the failure of SiC coatings. The SiC coatings are harder than the composite substrate. The fiber orientation has significant influence on the delamination of surface SiC coating. When the SiC coating is deposited parallel to the fiber orientation and interfacial delamination direction is along fiber direction, once delamination occurs, it inclines to propagate. When coating is prepared in other directions, the delamination inclines to stop. The present analyses show that, in application, a suitable combination of different fiber orientations can decrease the delamination of coating for better performance.

## Acknowledgments

X. Feng gratefully acknowledges the support from the National Basic Research Program of China (Grant No. 2015CB351904), National Natural Science Foundation of China (Grant Nos. 11222220, 11320101001, 11227801). W.X. Zhang acknowledges the support from National Natural Science Foundation of China (Grant Nos. 11172227, 11021202, 10902081) and 973 project (2013CB035701).

## References

- [1] Padmavathi N et al. Carbon fiber reinforced silicon carbide mini-composites-solution approach. *J Mater Process Technol* 2008;204(1–3):434–9.
- [2] Fang Xufei, Liu Fangsheng, Su Hengqiang, Liu Bin, Feng Xue. Ablation of C/SiC, C/SiC-ZrO<sub>2</sub> and C/SiC-ZrB<sub>2</sub> composites in dry air and air mixed with water vapor. *Ceram Int* 2014;40(2):2985–91.
- [3] Hoerner A, Vierhaus J, Burte EP. Chemically vapor-deposited silicon carbide films for surface protection. *Surf Coat Technol* 1998;100(1–3):149–52.
- [4] Cheng LF et al. Effect of coating defects on oxidation behavior of three dimensional C/SiCcomposites from room temperature to 1500 °C. *J Mater Sci* 2002;37(24):5339–44.
- [5] Goujard S, Vandenbulcke L, Tawil H. The oxidation behavior of 2-dimensional and 3-dimensional C/SiC thermostructural materials protected by chemical-vapor-deposition polylayers coatings. *J Mater Sci* 1994;29(23):6212–20.
- [6] Evans AG, Hutchinson JW. The thermomechanical integrity of thin-films and multilayers. *Acta Metall Mater* 1995;43(7):2507–30.
- [7] Fang Xufei, Jia Jingmin, Feng Xue. Three-point bending test at extremely high temperature enhanced by real-time observation and measurement. *Measurement* 2015;59:171–6.
- [8] Youjun G et al. Microstructure and mechanical properties of three-dimensional needled C/SiC composite. *J Chin Ceram Soc* 2008;2:144–9.
- [9] Bobet JL, Lamon J. Thermal residual-stresses in ceramic-matrix composites. 1. Axisymmetrical model and finite-element analysis. *Acta Metall Mater* 1995;43(6):2241–53.
- [10] Dalmaz A et al. Elastic moduli of a 2.5D C-f/SiC composite: experimental and theoretical estimates. *Compos Sci Technol* 2000;60(6):913–25.
- [11] Chamis CC. Mechanics of composite-materials - past, present, and future. *J Compos Tech Res* 1989;11(1):3–14.
- [12] Suo ZG. Singularities, interfaces and cracks in dissimilar anisotropic media. *Proc R Soc London Series A-Math Phys Eng Sci* 1873;1990(427):331–58.
- [13] Rice JR. A path independent integral and the approximate analysis of strain concentration by notches and cracks. *J Appl Mech* 1968;35(2):379–86.